Rate Coefficients for the Reactions of Hydroxyl Radicals with Methane and Deuterated Methanes

Tomasz Gierczak,[†] Ranajit K. Talukdar, Scott C. Herndon,[‡] Ghanshyam L. Vaghjiani,[§] and A. R. Ravishankara*[,‡]

National Oceanic and Atmospheric Administration, Aeronomy Laboratory, 325 Broadway, Boulder, Colorado 80303, and Cooperative Institute for Research in Environmental Sciences University of Colorado, Boulder, Colorado 80309

Received: November 21, 1996; In Final Form: February 11, 1997[⊗]

The rate coefficients for the reaction of OH with CH_3D (k_1), CH_2D_2 (k_2), CHD_3 (k_3), CD_4 (k_4), and CH_4 (k_5) as well as that of OD with CH_4 (k_6) have been measured using the pulsed photolytic production of OH followed by its detection via pulsed laser induced fluorescence. k_1-k_4 and k_6 were measured between ∼220 and ∼415 K, while k_5 was measured down to 195 K. The measured rate coefficients do not strictly obey the Arrhenius expression. However, below 298 K, they can be represented by the expressions (in cm^3 $molecule^{-1}$ s^{-1}): $k_1 = (3.11 \pm 0.44) \times 10^{-12} \exp[-(1910 \pm 70)/T]$; $k_2 = (2.3 \pm 1.2) \times 10^{-12} \exp[-(1930 \pm 250)/T]$; $k_3 = (1.46 \pm 0.22) \times 10^{-12} \exp[-(1970 \pm 70)/T]$; $k_4 = (1.00 \pm 0.22) \times 10^{-12} \exp[-(2100 \pm 120)/T]$; $k_5 = (1.88 \pm 0.11) \times 10^{-12} \exp[-(1695 \pm 30)/T]$; $k_6 = (1.68 \pm 0.12) \times 10^{-12} \exp[-(1640 \pm 40)/T]$. The obtained values of the rate coefficients and kinetic isotope effects are compared with values previously measured or calculated by other groups. The atmospheric implications of this data are briefly discussed.

Introduction

Methane is one of the most important and the most abundant trace organic gases in the atmosphere. It is one of the main reactants for the OH radical, which is the primary oxidant in the troposphere. Hence, CH_4 controls the abundance of OH in the troposphere. Oxidation of methane leads to ozone production. The importance of methane increases in the remote, clean troposphere, where it could be practically the only hydrocarbon. Because it absorbs well in the atmospheric infrared window and because of its large abundance, methane is one of the primary greenhouse gases contributing as much as 20% to the radiative forcing of the industrial atmosphere.[1] Transport of methane from the troposphere to the stratosphere, followed by its oxidation, provides the stratosphere with a large fraction of the water vapor. In addition, oxidation of methane in the presence of sufficient concentrations of nitrogen oxides leads to further production of OH and, hence, acts as an amplifier of HO_x species. For these reasons, methane is considered one of the most important constituents of the Earth's atmosphere.

Methane is produced by natural and human influenced biological activity as well as via fossil fuel usage.[2,3] Our ability to predict the future abundance of CH_4 in the atmosphere requires a quantitative knowledge of the sources and sinks of this molecule. The major process for the removal of methane from the atmosphere is its reaction with the OH radical. Other minor pathways include soil uptake. Because the atmospheric concentration of CH_4 is very well measured and its main process, i.e., its reaction with the OH radical, is quantified, the total flux of CH_4 into the atmosphere is reasonably well established. However, quantification of the individual sources of CH_4 remains elusive. The reason for this difficulty is the diffuse nature of the sources, whose emissions are individually small and variable in time. One of the approaches employed to constrain the source strengths has been to use isotopic signatures of various emissions and the isotopic composition of the atmospheric methane.[2−5] It has been suggested that the use of deutero-isotopomers of methane will potentially yield more information than the ^{12}C, ^{13}C isotopomers.[4] One piece of information that is essential for this exercise is the atmospheric isotopic fractionation of methane, which is almost completely due to the differences in the rate coefficients for the reactions of OH with different isotopomers. This method has been successfully employed using ^{12}C, ^{13}C, and ^{14}C isotopomers. However, in these cases, the atmospheric fractionation is very small. On the other hand, D to H substitution in the methanes leads to larger differences in the fractionation and the differences in these abundances have been recently measured.[4,6,7] One of the major pieces of information needed for an analysis of methane budget using the measurements of isotopomers is accurate rate coefficients for the reaction of OH with deuterated methanes relative to that for the OH + CH_4 reaction at atmospheric temperatures.

The rate coefficient for the reaction of OH with CH_4 is also needed to quantify the OH production in the lower stratosphere and upper troposphere, where the temperatures are often below 200 K, and where the methane oxidation acts as an amplifier of HO_x. Rate coefficients at such low temperatures for the reaction of OH with CH_4 are currently poorly defined. Further, CD_4 has been used as a tracer of atmospheric motion and its lifetime is needed to evaluate the time scales over which it is a conserved tracer.

In addition to their importance in the atmosphere, the OH+ CH_4 reaction has been a test bed for evaluating chemical kinetic theories and evaluating the capabilities to compute rate coefficients. Isotopically labeling the reactant does not change the potential energy surface for the reaction and, hence, provides an opportunity to test the ability of theorists to calculate rate

* Author to whom the correspondence should be addressed at: NOAA, R/E/Al-2, 325 Broadway, Boulder, CO 80303.

[†] On leave from Department of Chemistry, Warsaw University, ul. Zwirki i Wigury 101, 02-089 Warsaw, Poland.

[‡] Also associated with the Department of Chemistry and Biochemistry, University of Colorado, Boulder, CO 30809.

[§] Hughes STX, Phillips Laboratory, PL/RKFT, 10E. Saturn Blvd., Edwards AFB, CA 93524.

[⊗] Abstract published in *Advance ACS Abstracts,* April 1, 1997.

S1089-5639(96)03892-3 CCC: $14.00

constants. The reaction of OH with methane provides a large number of isotopic variants to test the calculations.

Because of the above reasons, the rate coefficients for the reactions of OH with all five H/D isotopomers of methane have been measured. The OD radical was also used in place of OH to investigate the secondary isotope effect in the reaction of hydroxyl radical with methane (CH_4). Such a variation is also a good way to assess possible systematic errors.

In this paper we describe our measurements of the rate coefficients for reactions 1−6, between ∼200 and 400 K.

$$OH + CH_3D \rightarrow H_2O + CH_2D \text{ and } HDO + CH_3; \quad k_1 \quad (1)$$

$$OH + CH_2D_2 \rightarrow H_2O + CHD_2 \text{ and } HDO + CHD_2; \quad k_2 \quad (2)$$

$$OH + CHD_3 \rightarrow H_2O + CD_3 \text{ and } HDO + CHD_2; \quad k_3 \quad (3)$$

$$OH + CD_4 \rightarrow HDO + CD_3; \quad k_4 \quad (4)$$

$$OH + CH_4 \rightarrow H_2O + CH_3; \quad k_5 \quad (5)$$

$$OD + CH_4 \rightarrow HDO + CH_3; \quad k_6 \quad (6)$$

The technique of pulsed photolysis−laser-induced fluorescence was employed to measure the rate coefficients k_1−k_6 as a function of temperature.

Experiments

The pulsed photolysis−(pulsed) laser-induced fluorescence (PP-PLIF) apparatus employed in this study has been used in our laboratory to measure OH reaction rate constants for many years and most recently in a similar investigation of the reactions of OH with H_2, HD, and D_2.[8] A detailed description of the apparatus, data acquisition methodology, and data analysis technique are given elsewhere.[8−10] Some modifications were carried out to the existing apparatus to minimize the use of the expensive isotopes and measure rate constants down to 195 K. Only the modifications specific to this study and certain details essential for understanding the present measurements are given here.

All experiments were carried out under pseudo-first-order conditions in hydroxyl radicals by maintaining the concentrations of methanes much larger than that of initially produced radicals ([methane] ≫ $[OH]_0$ or $[OD]_0$); hence, the concentration of methane was essentially constant during the course of the reaction. The temporal profiles of OH or OD in the reactor produced by pulsed photolysis were measured by monitoring their LIF signal, $S(t)$, as a function of reaction time t. The detection sensitivity for OH and OD was $\sim 1 \times 10^8$ cm^{-3}, in 100 Torr of He, when signals from 100 laser shots were averaged. In the presence of methanes, the LIF signal was degraded (due to the quenching of the excited OH/OD by methanes) significantly. For example, at the highest concentration of the methane ($\sim 9 \times 10^{16}$ cm^{-3}) used here, the detection sensitivity was $\sim 1 \times 10^9$ cm^{-3} for averaging 100 laser shots. Yet, the signal to noise ratios were excellent (S/N ≥ 100) when $[OH]_0$ was $\sim 1 \times 10^{11}$ cm^{-3} such that the temporal profiles were well-defined and the calculated loss rate constants were precise.

The LIF signal followed the first order differential equation:

$$\frac{d \ln S(t)}{dt} = -k_i[X_i] + k_d = k' \quad (I)$$

where $i = 1-6$, X_i is the methane reactant in that reaction, k_i is the rate coefficient for reaction i, and k_d is the first-order rate coefficient for loss of OH or OD in the absence of the methane due to reaction with impurities in the bath gas and diffusion out of the detection zone. The reaction time, t, was equal to the delay between the photolysis pulse (which generated the OH/OD reactant) and the probe pulse (which detected these radicals). The temporal profiles of the LIF signals were fitted to ln $S(t)$ vs t data (eq I) using a weighted (according to the square of the reciprocal of the standard deviation of the mean signal) linear least-squares analysis routine to extract k'. The second-order rate coefficients were obtained by measuring the first-order rate constant k' at various concentrations of methanes and fitting the variations of k' with $[X_i]$ to straight lines by using a weighted (according to the precision in k') linear least-squares analysis.

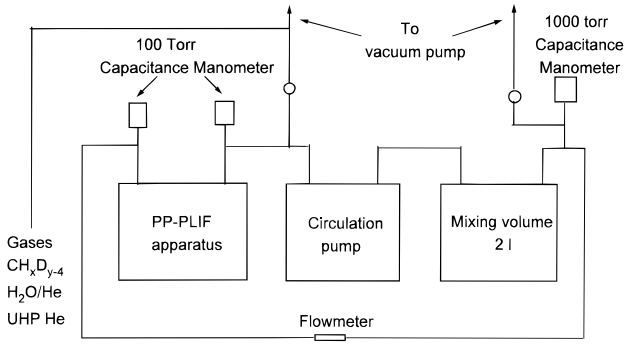

Figure 1. Schematic diagram of the recirculation system used to measure the rate constants for OH reactions with methane isotopomers.

Since the deuterated methanes are expensive, we employed a recirculation system (described below) to minimize their use. The recirculation system reduced methane use by factors of 20−50 compared to the conventional pump out configuration, where the gases are discarded after passing through the reactor once. The gas mixture used in the circulation system has to be stable with respect to thermal and wall-catalyzed decomposition under the experimental conditions we employed. Water and N_2O were chosen as the photolytic precursors for OH because they are stable compounds and do not isotope exchange with deuterated methanes under our experimental conditions. Further, both H_2O and N_2O can be photolyzed at wavelengths where methane does not absorb. Thus, we could completely avoid photolysis of methane while producing OH.

A schematic of the recirculation system and its connections to the reactor is shown in Figure 1. The main components of the recirculation system are a diaphragm circulation pump and mixing/ballast volume (2 L). The diaphragm pump was made of stainless steel and Teflon components and did not produce impurities or react with any of the gases that were recirculated. The temperature-controlled reaction cell, described in detail elsewhere,[8−12] was connected in series with the recirculation system. The total volume of the circulation system was ∼2.5 L, approximately 15 times the volume of the reactor. Also, because a very small volume of the reactor, <10 cm^3, was photolyzed by each pulse and the photolyzed volume was completely mixed in with the rest of the gas in the ballast, there was no significant depletion of the reactants or the buildup of products in the recirculating gas mixture.

The circulation system was operated in the following way: (1) the entire system (reactor, the pump, the ballast, and all the connecting components) was evacuated; (2) a known pressure of one of the methane isotopomer was introduced; (3) photolytic precursor and the diluent gas were added to bring the pressure up to ∼120 Torr; (4) the gas mixture was circulated for a few minutes to completely mix the gases; (5) OH/OD radical was produced via photolysis and its temporal profile was measured while circulating the gas mixture; (6) the circulation pump was

stopped, a fraction of mixture pumped out, and further diluted with the bath gas to bring the total up to the original pressure; (7) the new diluted mixture was circulated for a few minutes and another OH/OD temporal profile measured; (8) the dilution procedure was repeated a few times to measure k' at different (between two and six) concentrations of the methane. The concentration of methane in each mixture was calculated from its initial concentration, obtained by pressure measurements, and consecutive dilutions. A small fraction of the circulating gas mixture was periodically withdrawn and checked for impurities (products of the reactions and other compounds) via gas chromatographic analysis (GC). No changes in impurity levels were detected.

To check for systematic errors, three sources of hydroxyl radicals were used during the course of this investigation: (1) the photolysis of water vapor between 165 and 185 nm by the Xe flash lamp; (2) 193 nm ArF laser photolysis of N_2O followed by reaction of $O(^1D)$ with water; (3) Xe flash lamp photolysis of N_2O to generate $O(^1D)$ followed by reaction with methane. The last source was primarily used to measure k_6 at low temperatures (195−223 K), where the vapor pressure of water is too low to be used as an OH photolytic precursor. We generated OD radicals by replacing H_2O with D_2O.

The rate coefficients for the reaction of OH and OD with CH_4 were also measured using the conventional slow flow conditions. Linear gas flow velocities through the reactor in these experiments were 5−12 cm s^{-1}. Thus, the reaction zone, defined as the volume where the photolysis and the probe beams overlap, was replenished with a fresh mixture before each photolysis pulse. The concentration of CH_4 in these experiments was determined from the measured flow rates of CH_4, the buffer gas, and the photolyte/diluent mixture (using calibrated electronic mass flow meters) and the total pressure (measured by capacitance manometers).

The concentration of deuterated methanes in the gas mixture was verified by GC analysis. The GC signals were calibrated using several standard mixtures of CH_4 in He, prepared manometrically.

The temperature of the gases flowing through the reaction zone was measured by a retractable thermocouple and was estimated to be accurate to ±0.5 K.

Samples. Since reactions 1−6 are relatively slow, even traces of impurities such as unsaturated hydrocarbons, which react very rapidly with OH, can introduce large errors if they are present in the methane samples. Therefore, the accurate knowledge of the purity of the samples is essential. Ultra high purity (>99.999%, <1 ppmv of total of unsaturated hydrocarbons) CH_4 was obtained from Matheson Gas Products Ltd. CHD_3, CH_2D_2, CHD_3, and CD_4 were purchased from Isotec Inc. Each sample was analyzed using a GC equipped with a flame ionization detector and megabore capillary column GS-Al (PLOT). The measured levels of the impurities in the samples obtained from the vendors are shown in Table 1. Since the levels of hydrocarbons were undetectably low in the CH_4 and CD_4 samples, they were used without further purification. The CD_4 sample was reported by the vendor to contain 59 ppmv of CO. This sample was analyzed using an FTIR and found to contain less than 15 ppmv of CO. We used two different samples of CH_3D with differing levels of reactive impurities. In sample 1, only ethane and ethene were detected. Their concentrations were such that all the reactive impurities together would not affect the measured values of k_1 even at the lowest temperature. Therefore, they were used without further purification. The level of impurities in sample 2 was larger. However, they were not large enough to affect the rate coefficients at $T \geq 298$ K. Therefore, this sample was used only at temperatures above 298 K. Large concentrations of ethene and propene were detected in the CH_2D_2 and CHD_3 samples. In the CHD_3 sample, a large amount of ethane was also found. A short column (50 cm long × 0.6 cm diameter) packed with concentrated $H_2SO_4/AgNO_3$ deposited on Chromosorb WHP was used to remove unsaturated hydrocarbons from these samples. For each experiment the deuterated methane sample was passed through the purification column and the eluting gas was checked for the presence of unsaturated compounds using GC analysis. If an unacceptable level of ethene or propene was seen, the purification column was repacked. The CHD_3 sample was also passed through a column packed with Carbosieve S II to reduce the levels of ethane to less than 50 ppmv. This process also completely removed larger alkanes. The levels of impurities in the samples that were used for rate constant measurements are included in Table 1. The isotopic purities of CH_3D, CH_2D_2, CHD_3, and CD_4 samples were 98, 98, 99.6, and 99.8%, respectively. Isotopic purity of D_2O was 99.89%. UHP He, used as a carrier gas, was 99.9995% pure.

TABLE 1: Impurities Detected in the Samples of Methane and Deuterated Methanes Used in the Present Study

compound	impurity	original sample, ppmv	purified sample, ppmv
CH_4	none	<0.5 total	<0.5 total
CH_3D (sample 1)	Ar, O_2, N_2, CO_2	<150 total	<150 total
	ethane	23	*b*
	ethene	44	*b*
	propane	<10	*b*
	propene	<10	*b*
CH_3D (sample 2)	ethane	450	*c*
	ethene	112	*c*
	propane	55	*c*
	propene	15	*c*
CH_2D_2	ethane	70	<0.5
	ethene	630	<0.5
	propene	10	<0.5
CHD_3	ethane	1400	<50
	ethene	250	<0.5
	propane	300	<0.5
	propene	50	<0.5
CD_4	CO	59[a]	15
	N_2	23[a]	23
	Ar/O_2	<20[a]	<20
	CO_2	<20[a]	<20

[a] Analysis supplied by ISOTEC, Inc. [b] Used as supplied. [c] Used only for experiments at $T > 298$ K.

Results

The measured values of the rate coefficients k_1−k_6 are listed in Table 2, along with the experimental conditions employed for their determinations. The same data are also plotted in Figure 2 in the classical Arrhenius form, i.e., k (on a log scale) vs $1/T$. The figure shows not only the data obtained here but also the k_5 (between 223 and 422 K) determined previously in our laboratory.[11] Combining these two data sets is acceptable because essentially the same apparatus and procedures were used in both studies.

There are two major problems associated with measuring very small OH reaction rate coefficients using the technique employed here: (1) the presence of impurities in the samples and (2) secondary reactions which can deplete (and also possibly regenerate) OH via reactions other than the one being investigated. It is extremely important to pay attention to the purities of the samples and to check for occurrence of secondary reactions. These two factors are discussed for each of the reactions studied here.

TABLE 2: Summary of Experimental Conditions and Measured Values of Rate Coefficients of OD and OH Radicals with Methane and Deuterated Methanes

reaction	temp K	$[OH]_0$, 10^{10} molecules cm^{-3}	range of $[CH_xD_y]$, 10^{16} molecule,cm^{-3}	buffer gas/press., Torr	k_{bi}, 10^{15} cm^3 $molecule^{-1}$ s^{-1}	reaction	temp K	$[OH]_0$, 10^{10} molecules cm^{-3}	range of $[CH_xD_y]$, 10^{16} molecule, cm^{-3}	buffer gas/press., Torr	k_{bi}, 10^{15} cm^3 $molecule^{-1}$ s^{-1}
OD + CH_4[b]	420	10	0.5−4.9	He/100	46.16 ± 0.29		278	16[a]	0.81−9.38	He/100	3.28 ± 0.20
	420	3[a]	0.5−4.1	He/100	46.69 ± 0.64		273	7	1.02−9.15	He/100	2.84 ± 0.14
	420	30	0.5−7.5	He/100	47.47 ± 0.40		268	7	0.68−9.29	He/100	2.59 ± 0.13
	420	9	0.6−6.5	He/100	46.85 ± 0.63		263	17	0.92−9.42	He/100	2.16 ± 0.18
	380	10	0.5−6.6	He/100	27.44 ± 0.22		258	7	1.12−9.96	He/100	1.83 ± 0.14
	350	20	0.6−6.7	He/100	17.75 ± 0.24		253	7	1.44−11.09	He/300	1.60 ± 0.16
	325	10	0.8−7.8	He/100	11.70 ± 0.07		249	37	1.26−10.13	He/100	1.50 ± 0.05
	303	3	0.6−5.3	He/100	7.48 ± 0.18	OH + CH_2D_2[g]	354	10[a]	0.55−4.21	He/100	9.08 ± 0.54
	273	15	9.0−42.8	He/100	4.20 ± 0.03		324	1	0.39−3.33	He/100	5.59 ± 0.32
	273	16	7.9−36.7	He/100	4.14 ± 0.07		297	2[a]	0.84−5.06	He/100	3.53 ± 0.34
	250	16	7.0−35.7	He/100	2.30 ± 0.03		297	2	0.93−5.59	He/100	3.64 ± 0.44
	233	10	6.3−24.4	He/100	1.48 ± 0.03		270	6	0.90−5.15	He/100	1.60 ± 0.30
	233	3	2.3−10.8	He/100	1.50 ± 0.01	OH + CHD_3[b]	354	140[a]	0.60−6.83	He/100	5.64 ± 0.20
	233	10	3.1−16.2	He/100	1.43 ± 0.03		323	14[g]	0.60−5.90	He/100	3.28 ± 0.34
	223	4	0.8−7.6	He/100	1.09 ± 0.02		297	7.5	0.84−5.18	He/100	1.97 ± 0.04
OH + CH_4[b,c]	296	20	0.88−4.57	He/100	6.20 ± 0.16		295	10[g]	0.99−7.10	He/100	1.77 ± 0.10
	295	2	0.58−4.87	He/100	6.15 ± 0.26		293	6	2.19−12.43	He/100	1.71 ± 0.20
	295	2	0.37−5.15	He/100	5.90 ± 0.16		270	10[a]	1.40−8.40	He/100	1.02 ± 0.04
	295	1	0.53−5.04	He/100	5.85 ± 0.22	OH + CD_4[b]	413	3	0.44−7.63	He/100	9.79 ± 0.40
	295	1	0.53−5.50	He/100	6.02 ± 0.10		413	3	0.09−0.87	He/100	9.85 ± 0.40
	223	2	0.59−7.99	He/100	0.82 ± 0.42[d]		413	88	0.68−7.70	He/100	10.1 ± 0.1
	218	3	0.77−8.00	He/100	0.75 ± 0.07[d]		391	2[a]	0.74−6.56	He/100	6.97 ± 0.18
	213	2	1.37−8.71	He/100	0.63 ± 0.06[d]		380	3	0.52−6.21	He/100	5.77 ± 0.22
	206	10	1.50−8.28	He/100	0.49 ± 0.03[d]		357	2	0.81−8.13	He/100	3.67 ± 0.12
	200	1	0.98−8.49	He/100	0.40 ± 0.02[d]		346	4	0.70−9.12	He/100	2.95 ± 0.08
	195	1	0.98−8.49	He/100	0.36 ± 0.02[d]		333	2[a]	0.63−7.68	He/100	2.23 ± 0.05
OH + CH_3D[b,e]	422	21.5	0.25−1.99	He/100	37.4 ± 1.2		320	4	1.10−9.59	He/100	1.56 ± 0.18
	413	2	0.16−1.60	He/100	32.1 ± 2.7[f]		310	2[a]	0.86−8.28	He/100	1.32 ± 0.05
	403	2[a]	0.46−1.95	He/100	28.1 ± 1.6		300	16	0.62−8.94	He/100	0.87 ± 0.02
	391	2	0.19−2.08	He/100	23.89 ± 0.57[f]		299	5	0.72−10.53	He/100	0.86 ± 0.05
	376	12[a]	0.16−2.25	He/100	20.21 ± 0.76		296	88	1.46−10.01	He/100	0.84 ± 0.04[d]
	362	2.5[a]	0.41−3.37	He/100	15.64 ± 0.58[f]		296	18	1.04−6.12	He/100	0.85 ± 0.02
	353	1	0.29−2.43	He/100	13.57 ± 0.60[f]		289	5	1.36−11.21	He/300	0.66 ± 0.04
	343	3	0.32−2.45	He/100	11.43 ± 0.81		282	10	1.12−10.50	He/100	0.56 ± 0.06
	330	3[a]	0.18−3.72	He/100	9.35 ± 0.48		276	5	1.32−11.71	He/100	0.44 ± 0.02
	317	3	0.47−3.88	He/100	7.34 ± 0.14		269	11	1.56−12.60	He/100	0.39 ± 0.02
	307	4	0.51−7.88	He/300	6.15 ± 0.10		265	3[a]	1.34−10.66	He/100	0.33 ± 0.02
	298	3[a]	0.43−6.94	He/100	5.05 ± 0.18		259	11	1.75−11.59	He/100	0.27 ± 0.02
	298	31	0.98−7.59	He/100	5.06 ± 0.29		250	12	1.37−16.10	He/100	0.23 ± 0.03[h]
	291	31	0.88−10.32	He/100	4.48 ± 0.12		244	21	0.94−7.34	He/100	0.19 ± 0.02[d,h]
	286	32	0.60−8.66	He/100	3.82 ± 0.20						

[a] Half of the full flash energy. [b] The photodissociation of H_2O was used as the OH source. [c] The photodissociation of N_2O followed by the reaction of $O(^1D)$ with methane was used as the OH source for 223−195 K measurements. [d] Typical slow flow condition. [e] All experimental values corrected for the presence of 44 ppmv of ethene. [f] Experimental value corrected for the presence of 650 ppmv of ethane, 112 ppmv of ethene, 55 ppmv of propane and 15 ppmv of propene. [g] The photodissociation of N_2O at 193 nm followed by the reaction of $O(^1D)$ with H_2O was used as a OH source. [h] Experimental values corrected for the presence of 59 ppmv of CO. All uncertainties are 2σ and do not include estimates of systematic errors or errors due to corrections for impurity reactions.

The short chain hydrocarbons were the most significant impurities in our samples (see Table 1). Of these, the unsaturated hydrocarbons which react with OH with rate coefficients close to 1×10^{-11} cm^3 $molecule^{-1}$ s^{-1} at 298 K were of most concern. Saturated hydrocarbons are less reactive toward OH (rate coefficients of 10^{-12}−10^{-13} cm^3 $molecule^{-1}$ s^{-1})[13]. However, if they are present in large quantities they can also contribute significantly. We never detected any hydrocarbons larger than C_3H_8.

The simplest way to avoid influence of secondary reactions is to prevent formation of reactive free radicals via the photolysis pulse and to maintain a very large ratio of the concentration of methanes to that of the initial OH. Smaller rate coefficients require larger ratios of the concentrations of the reactant to initial OH to minimize secondary reactions. As shown in Table 2, the initial concentration of OH was approximately 10^5 times smaller than those of the methanes. We employed photolysis wavelengths where methane (or its isotopomers) does not absorb. Therefore, large concentrations of free radicals such as CH_3 and H were not generated by the photolysis of methanes. The easiest way to test for secondary reactions is to vary the initial concentration of OH. The secondary reactions of OH with the methyl radical, produced in reactions 1−6, enhances the measured rate constant. The influence of such reactions has been discussed in our earlier paper[11] and will not be repeated here. Other parameters which can shed light on secondary reactions are the photolysis fluence, gas flow velocity, and system pressure. In the following few paragraphs we briefly mention the tests that were carried out along with an accounting for the presence of the impurities.

OH + CH_3D (k_1). The rate coefficient for reaction 1, k_1, was measured by producing OH via the photodissociation of water by a Xe flash lamp. Other sources of OH were not used. The initial concentration of OH was varied by a factor of nearly 40 and the measured rate coefficients did not change. The measured value of k_1 did not change when pressure was varied by a factor of 3, linear flow rate by a factor of 3.5, and the flash lamp energy by a factor of 4. Therefore, we are confident that the measured values of k_1 were not influenced by secondary reactions.

Two samples of CH_3D, with differing levels of impurities, were used in this study. The exact concentrations of the

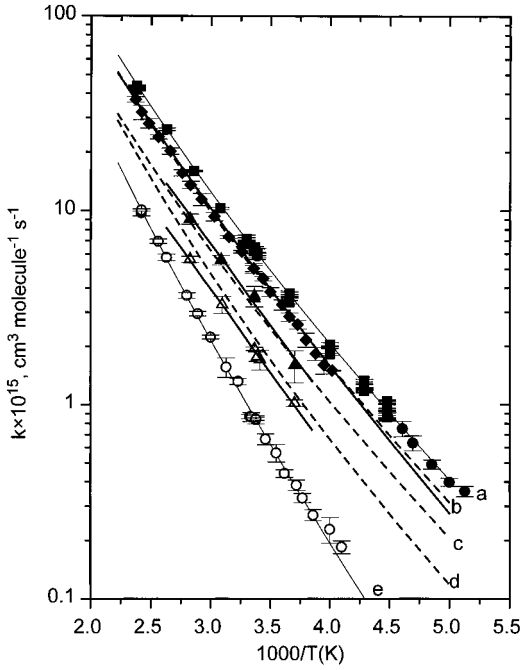

Figure 2. Arrhenius plots of the rate coefficients for the reactions of OH with methane and its deuterated analogs: (a) CH_4, squares from Vaghjiani and Ravishankara,[11] circles, this work; (b) CH_3D, diamonds; (c) CH_2D_2, triangles; (d) CHD_3, open triangles; (e) CD_4, open circles. Solid lines represent the best fits to the experimental data using either a three-parameter equation $k(T) = AT^n \exp(-E_a/RT)$ for CH_4, CH_3D, CD_4, or an Arrhenius equation $k(T) = A \exp(-E_a/RT)$ for CH_2D_2 and CHD_3; Dashed lines were calculated from the equation $k_{CH_xD_y}(T) = ((x/4)k_{OH+CH_4}) + ((y/4)k_{OH+CD_4})$ (for explanation see text).

impurities, listed in Table 1, were determined via GC analyses. The measured rate coefficients were corrected for the loss of OH via reactions with these impurities. Sample 1 contained 44 ppmv of ethene as the major reactive impurity. The isotopic composition of the ethene was not known. Assuming this impurity to be C_2H_4 and using the known rate coefficient for the reaction of OH with C_2H_4, we corrected the measured values of k_1. The correction ranged from 0.8% at 376 K to 25% at 249 K. Sample 2 was used only to measure k_1 at $T > 298$ K. The corrections in this case ranged from 3.5% at 413 K to 16% at 317 K. Note that even if the ethene contains D atoms, the rate coefficient for its reaction with OH is unlikely to be different from that for the reaction of OH with C_2H_4. Therefore, the uncertainty in the correction is expected to be quite small.

OH + CH_2D_2 (k_2). For measuring k_2, the OH radicals were generated via laser photolysis of N_2O to produce $O(^1D)$, followed by its reaction with H_2O (see Table 2). Because of concerns with the possible buildup of reactive impurities, the circulating mixture was diluted only once and, thus, two different concentrations of CH_2D_2 were generated for each fill. Unsaturated hydrocarbon impurities, such as ethene and propene, were removed using the purification column described earlier and their levels were <0.5 ppmv. Ethane was not removed, but its contribution to the measured rate coefficient was calculated to be less than 1%. The level of impurities in the gas mixture circulating through the reactor was checked by GC analysis for each new mixture.

OH + CHD_3 (k_3). Two sources of OH radicals, Xe flash lamp photolysis of H_2O and 193 nm laser photolysis of a mixture of N_2O and H_2O, were used to measure k_3. The measured rate coefficient did not depend on the OH source. As in the case of CH_2D_2, only two OH temporal profiles were measured for each fill of the recirculation system. Again, all unsaturated hydrocarbons and most saturated hydrocarbons were removed using the purification column as discussed earlier. The sample had about 50 ppmv of ethane even after purification; however, it contributed less than 1% to the measured rate coefficient even at the lowest temperature.

OH + CD_4 (k_4). This is the slowest rate coefficient reported in this study and, hence, likely to be influenced by systematic errors. Therefore, a large number of tests were performed. The hydroxyl radicals were generated via the flash lamp photolysis of H_2O. The pressure was varied by a factor of 3, the flash lamp energy altered by a factor of 4, and the $[OH]_0$ changed by a factor of 30; yet, the measured rate coefficient was unaffected by these changes. In addition to using the recirculation system, the conventional pump out system was also employed at 296 and 244 K; the measured values were the same as in the recirculation system.

The only detected reactive impurity in our sample of CD_4 was CO. The contribution of CO to the measured loss is small even at 250 and 244 K. The corrections amounted to ~2%. The isotopic purity was high enough that any contribution of CH_4 and partially deuterated methanes to the measured values of k_4 were negligible (<2%).

OH + CH_4 (k_5). Both the conventional (slow-flow pump out) and recirculation configurations were employed to measure k_5. The recirculation system, where OH was produced by flash photolysis of H_2O vapor, was used to measure k_5 at room temperature. Those measurements served as a check of the circulation system, as k_5 at 298 K is well established. Experimental data acquired using the recirculation system agrees very well with that from the conventional flow out method. In one set of experiments at 295 K, the concentration of CH_4 flowing through the recirculation system was measured by GC analysis and we obtained $k_5 = (6.15 \pm 0.26) \times 10^{-15}$ cm^3 molecule^{-1} s^{-1}, in excellent agreement with that measured previously (3.5% higher than the recommended value [DeMore, ref 13]). The sample of methane was sufficiently pure that it was not necessary to correct k_5 for any impurities.

The conventional slow flow, pump out, configuration was used to measure the OH rate coefficients at very low temperatures between 250 and 195 K. Because the water vapor pressure at these temperatures are low, we used the flash lamp photolysis of N_2O followed by the reaction of $O(^1D)$ with CH_4. The total mass flow rate and pressure were typically 700 STP cm^3 min^{-1} and 100 Torr, respectively. We also measured k_5 at 298 K using this source of OH to be $k_5 = (6.20 \pm 0.16) \times 10^{-15}$ cm^3 molecule^{-1} s^{-1}, essentially the same as the value measured using other sources. The agreement shows that $O(^1D) + CH_4$ is a good source of OH and can be used with confidence at lower temperatures.

OD + CH_4 (k_6). The conventional slow flow, pump out, configuration system was employed to measure k_6 between 420 and 223 K in 100 Torr of helium. The measured values of the second-order rate coefficients were found to be independent of flow velocity (2.5−7 cm s^{-1}) and $[OD]_0$ (a factor of 10). The k_6(298 K) was measured to be $(6.77 \pm 0.18) \times 10^{-15}$ cm^3 molecule^{-1} s^{-1}. As in the case of k_5, it was not necessary to correct k_6 for impurities.

The major sources of systematic errors are the knowledge of the concentration of methanes and corrections to the measured values because of the presence of reactive impurities. We estimate that the concentrations of the excess reagents were known to better than 5% and the uncertainties due to the corrections ranged from 5 to 10%, depending on the level of impurities. These estimated systematic uncertainties were added, in quadrature, to the precision of the measurements

TABLE 3: Rate Parameters for the Reaction of OH Radical with Methane and Deuterated Methanes Derived from the Present Work for Atmospheric Calculations[a]

molecule	A,[b] K	$E/R \pm (\Delta E/R)$, K	T range, K	$k(298)$[c]	$f(298)$[d,e]
CH_4[f]	1.68	1640 ± 40	223−303	6.84	1.06
CH_4	1.88	1695 ± 30	195−303	6.35	1.06
CH_3D	3.11	1910 ± 70	249−298	5.12	1.1
CH_2D_2	2.30	1930 ± 250	270−354	3.54	1.14
CHD_3	1.46	1970 ± 80	270−354	1.94	1.14
CD_4	1.00	2100 ± 120	244−300	0.870	1.1

[a] Derived using data obtained at $T < 303$ K. [b] Unit for A is 10^{-12} cm^3 molecule^{-1} s^{-1}. [c] Unit for k is 10^{-15} cm^3 molecule^{-1} s^{-1}. [d] $f(T) = f(298)\langle\exp|(\Delta E/R)((1/T) - (1/298))|\rangle$. [e] Our uncertainties are 2σ and include estimates of systematic errors as discussed in the text. [f] OD + CH_4 experiment.

(derived from the least-squares analyses) to estimate the overall uncertainties.

For use in atmospheric modeling, a weighted least-squares fit to the linearized Arrhenius equation

$$\ln [k(T)] = \ln (A) - \left(\frac{E}{R}\right)\frac{1}{T} \qquad \text{(II)}$$

was carried out for each rate coefficient k_1 through k_6 using values measured at and below 298 K. The obtained results are shown in Table 3. The uncertainties in the parameters are represented in the form adopted by the data evaluation panel NASA/JPL[13] and IUPAC:[14]

$$f(T) = f(298)\left\{\exp\left|\frac{\Delta E}{R}\left(\frac{1}{T} - \frac{1}{298}\right)\right|\right\} \qquad \text{(III)}$$

where $f(T)$ and $f(298)$ are uncertainties in the rate coefficients at 298 K and T, respectively, ΔE is not the uncertainty in the activation energy E but a parameter derived to estimate the uncertainty in the value of the rate coefficient at temperature T. The uncertainties are given at the 95% confidence limit and include estimated systematic errors. The value of k(298 K) was derived by using the values measured at temperatures close to 298 K and an activation energy derived in this work. When necessary, the A values have been slightly adjusted to reproduce the k(298 K).

The Arrhenius plots for CH_4, CH_3D, and CD_4 are slightly curved over the entire temperature range and our data are better represented by the three-parameter equation ($AT^n \exp(-E/T)$). The results of such three parameter fits are shown in the Table 4. For accurate interpolation of k_5 in the temperature range of our measurements, the three-parameter expression, rather than the conventional Arrhenius expression, should be used.

Comparison with the Previous Work

The 298 K rate coefficients and the Arrhenius parameters for the OH reactions obtained in the present work, along with those from previous studies, are summarized in Table 4.

There are two previous reports of k_1, one by Gordon and Mulac[15] at 416 K and one by DeMore[16] between 290 and 360 K. We are the first to report k_1 in the atmospherically important temperature region (below 298 K). Gordon and Mulac measured k_1 using the pulse radiolysis of water vapor to produce OH and 308.7 nm absorption to detect it. Their value of $(3.65 \pm 0.17) \times 10^{-14}$ cm^3 molecule^{-1} s^{-1} at 416 K is in good agreement with (about 6% higher than) our value. DeMore measured k_1 relative to the rate coefficients for the reactions of OH with HFC-134a (CF_3CFH_2) and HCFC-141b (CH_3CCl_2F). He preferred the values obtained using HFC-134a. These values of DeMore are slightly higher than ours (7% at 298 K and 4% at 360 K) but within the error limits of the measurements. The Arrhenius parameters derived from DeMore's data are also in good agreement with ours.

Gordon and Mulac have also measured k_2 and k_3 at 416 K. Their value of k_2 is 40% higher than that measured here. On the other hand, their value of k_3 at 416 K is about 13% lower than ours. These authors did not present the chemical analyses of their samples and it is difficult to judge the accuracy of their measurements. We are the first to report k_2 and k_3 as a function of temperature.

Dunlop and Tully[17] measured k_4 between 293 and 800 K using an experimental technique very similar to ours. Results

TABLE 4: Comparison of OH Reaction Rate Coefficients with Previous Work

molecule	A[a]	n	$E/R \pm (\Delta E/R)$, K	temp range, K	$k(298)$,[a] 10^{15}	$k(416)$,[a] 10^{15}	technique[b]	reference
CH_4[c]	7.44 ± 10^{-21}	2.94	897 ± 84	420−223	6.84 ± 0.41	43.2 ± 2.6	FP-LIF	this work
CH_4	1.85×10^{-20}	2.82	987 ± 6	420−195	6.40 ± 0.38	41.9 ± 2.5	FP-LIF	this work[d]
	9.65×10^{-20}	2.58	1082	800−293	6.18	41	PLP-LIF	17
	$(2.56 \pm 0.53) \times 10^{-12}$		1765 ± 146	343−233	6.34 ± 0.56	36.8 ± 1.1	PLP-LIF	19
	$4.0^{+1.6}_{-1.3} \times 10^{-12}$		1944 ± 114	378−278	5.87 ± 0.98	37.4 ± 1.2	DF-RF	18
	6.3×10^{-12}		2030 ± 100	330−260	6.93 ± 2.8	47.9 ± 13	FP-RF	31
				298	6.11 ± 0.2[e]		PLP-LIF	20
						54.8 ± 1.6	PR-AS	15
				298−178	7.6 ± 0.3		PLP-LIF	21
	2.65×10^{-12}		1800 ± 150	400−223	6.3 ± 0.6	35.0 ± 5.5		13
CH_3D	1.07×10^{-17}	1.87	1332 ± 20	420−249	5.12 ± 0.51	34.4 ± 3.44	FP-LIF	this work
						36.5 ± 1.7	PR-AS	15
	3.21×10^{-12}		1897	358−298	5.52	33.6	RR	16[f]
	4.67×10^{-12}		2003	361−293	5.62	37.9	RR	16[g]
	3.5×10^{-12}		1950 ± 200	298−249	5.0 ± 0.75	32.2 ± 7.0		13
CH_2D_2	2.18×10^{-12}		1926 ± 250	354−270	3.54 ± 0.50	21.3 ± 2.98	FP-LIF	this work
						29.9 ± 1.6	PR-AS	15
CHD_3	1.46×10^{-12}		1972 ± 80	354−270	1.94 ± 0.27	12.8 ± 1.79	FP-LIF	this work
						11.1 ± 0.5	PR-AS	15
CD_4	5.65 ± 10^{-21}	3.01	1545 ± 15	413−244	0.87 ± 0.09	10.5 ± 1.05	FP-LIF	this work
	8.70×10^{-22}	3.23	1334	800−293	0.97	10.2	PLP-LIF	17
						5.0 ± 0.2	PR-AS	15

[a] Units: cm^3 molecule^{-1} s^{-1}. [b] FP = flash photolysis, PLP = pulse laser photolysis, DF = discharge flow, PR = pulse radiolysis, RT = relative technique, LIF = laser-induced fluorescence, RF = resonance fluorescence, AS = absorption spectrophotometry. [c] OD + CH_4 experiment. [d] Fit does include experiments from ref 11. [e] The 292 K data was scaled to 298 K using an E/R of 1800. [f] Measured relative to HFC-134a. [g] Measured relative to HFC-141b. All errors are those quoted by the authors. Our uncertainties are 2σ and include estimates of systematic errors.

TABLE 5: Kinetic Isotope Effect Data (KIE[a] = A exp(B/T) for the Reaction of OH with Deuterated Methanes

molecule	$A \pm 2\sigma$	$B \pm 2\sigma$, K	temp range, K	KIE[b](298) $\pm 2\sigma$[c]	KIE[d](416) $\pm 2\sigma$[c]	reference
CH_3D	1.09 ± 0.10	49 ± 22	422−249	1.25 ± 0.14	1.22 ± 0.14	this work
					1.50 ± 0.16[e]	Gordon and Mulac[15]
					1.14 ± 0.11[f]	
	0.91 ± 0.33	75 ± 118	361−293	1.16 ± 0.07	1.08 ± 0.07	DeMore[16g]
	0.61 ± 0.21	184 ± 112	358−298	1.13 ± 0.07	0.95 ± 0.06	DeMore[16h]
CH_2D_2	1.39 ± 0.81	92 ± 140	354−270	1.81 ± 0.28	1.97 ± 0.30	this work
					1.83 ± 0.22[e]	Gordon and Mulac[15]
					1.39 ± 0.15[f]	
CHD_3	2.14 ± 0.48	126 ± 64	354−270	3.30 ± 0.50	3.27 ± 0.50	this work
					4.94 ± 0.54[e]	Gordon and Mulac[15]
					3.75 ± 0.35[f]	Gordon and Mulac[15]
CD_4	1.03 ± 0.10	573 ± 50	413−244	7.36 ± 0.88	3.99 ± 0.46	this work
					10.9 ± 1.1[e]	Gordon and Mulac[15]
					8.32 ± 0.71[f]	
CD_4	0.95 ± 0.03	598 ± 24	800−293	6.55 ± 0.83[i]	3.94 ± 0.35[j]	Dunlop and Tully[17]
CD_4[k]	1.07 ± 0.04	609 ± 14	2400−223	8.39 ± 0.54	4.53 ± 0.32	Melissas and Truhlar[24]

[a] KIE = $k_{OH+CH_4}/k_{OH+CH_xD_y}$. [b] KIE values were calculated using room temperature rate coefficients from Table 4. The A and B parameters reproduce these values to within ∼10%. [c] The quoted error σ = KIE × $[(\sigma/k)^2_{OH+CH_4} + (\sigma/k)^2_{OH+CH_xD_y}]^{1/2}$. [d] Calculated from Table 4. [e] Calculated using rate coefficients for OH with CH_xD_y at 416 K quoted in ref 15. [f] Calculated using Gordon and Mulac's rate coefficient for OH with CH_xD_y at 416 K and the rate coefficient for OH with methane from ref 13. [g] Measured relative to HFC-134a. [h] Measured relative to HFC-141b. [i] Experimental value at 293 K was scaled to 298 K. [j] Experimental value at 409 K was scaled to 416 K. [k] The fit was calculated by us using values for KIEs quoted in the ref 25 (Table XI).

from the present study agree with their values in the overlapping temperature region. Further, k_4 calculated at $T \leq 298$ K from an extrapolation of Dunlop and Tully's data is in excellent agreement with our measured values. The rate coefficients measured by Gordon and Mulac at 416 K is almost a factor of 2 lower than our value as well as that of Dunlop and Tully. Such a large discrepancy and, specifically, the lower value of Gordon and Mulac are hard to understand. To our knowledge, we are the first to report k_4 in the atmospherically important temperature region, i.e., at $T < 298$ K.

One of the goals of this study was to measure k_5 at the temperatures of the lower stratosphere and the upper troposphere. k_5 was also measured around 298 K to validate the recirculation system that was used for the studies of the isotopically labeled methanes. We have measured k_5 over a very limited temperature range, 223−195 K, and around 298 K. Therefore, the Arrhenius parameters reported in Tables 3 and 4 were obtained by combining the data of this study with those from our previous measurements using the same apparatus and procedures,[11] as discussed earlier.

Several groups[11,17−21] have recently reported k_5 at 298 K, as well as its variation with temperature.[11,17−19,21] The agreement between most of the studies is excellent. Sharkey and Smith[21] have measured k_5 below 223 K: at 216 and 178 K. For 178 K, they quote only an upper limit ($< 3 \times 10^{-16}$ cm^3 molecule^{-1} s^{-1}). Their value at 216 K is twice that measured here. Their 298 K values are also higher than all other recent measurements. Because of very high initial concentration of hydroxyl radicals employed by them, Sharkey and Smith carried out computer simulation of the OH temporal profiles to extract k_5. The corrections were less than 10%. As they pointed out, it is unlikely that the discrepancy is due to secondary reactions in their system. Thus, the origin of the difference is unclear.

Greiner,[22] as part of his original systematic studies of OH reactions, reported $k_6 = (8.0 \pm 0.3) \times 10^{-15}$ cm^3 molecule^{-1} s^{-1} at 300 K. This value is only ∼10% higher than that obtained in this work, even though his k_5 value is significantly higher. He had to employ quite high initial concentrations of OH and did not pay a great deal of attention to impurity levels. It should be noted, however, that he obtained excellent kinetics data for his era and accuracies of 10%, or lower, were not the main goals of his measurements.

Discussion

The reactions of hydroxyl radicals with alkanes proceed via abstraction of a hydrogen atom. The large kinetic isotope effect, the differences between k_4 and k_5, attests to this mechanism. The trend in reactivity with deuteration is interesting. Recently, we pointed out that the rate coefficient for the reaction of OH with HD is the algebraic average of the rate coefficients for the reactions of OH with H_2 and D_2.[12] We observe a very similar trend in the case of the deuterated methanes. The rate coefficients for the reactions of OH with CH_3D, CH_2D_2, and CHD_3 can be expressed as

$$k(\mathrm{OH}+\mathrm{CH}_x\mathrm{D}_y) = \left(x\frac{k_5}{4}\right) + \left(y\frac{k_4}{4}\right) \qquad \text{(IV)}$$

where $x = 1$, 2, and 3 and $y = 4 - x$. The calculated values at various temperatures are plotted in Figure 2 as dashed lines. For these calculations, the rate constants expressions for k_4 and k_5 given in Table 4 were used. As can be seen in the figure, for CH_3D and CH_2D_2, the agreement between the calculated and the measured values is excellent over the entire temperature range. This agreement can be interpreted, as in the case of OH + H_2/HD/D_2 reactions, as an indication that the reaction proceeds mostly via tunneling. The measured values of k_3 are about 15% lower than the predicted ones. This difference could be associated with the experimental error, especially because the data on k_3 are more uncertain. However, we cannot exclude the possibility that the composition of the methyl group can influence, albeit slightly, the rate coefficients for abstraction reactions.

From Figure 2 it can be seen that Arrhenius plots show an upward curvature at higher temperatures (clearly visible for CH_4, CH_3D, and CD_4). Many other bimolecular reactions have shown such a behavior. Transition state theory (TST) does predict non-Arrhenius behaviors when allowance is made for the variation of the vibrational partition functions with temperature even without quantum mechanical tunneling. If the rate coefficient is measured over a limited temperature range, especially at low temperatures, the experimentally measured activation energy can appear temperature independent. A comparisons of k_4 and k_5 show that activation energy at low temperatures (298−220 K)

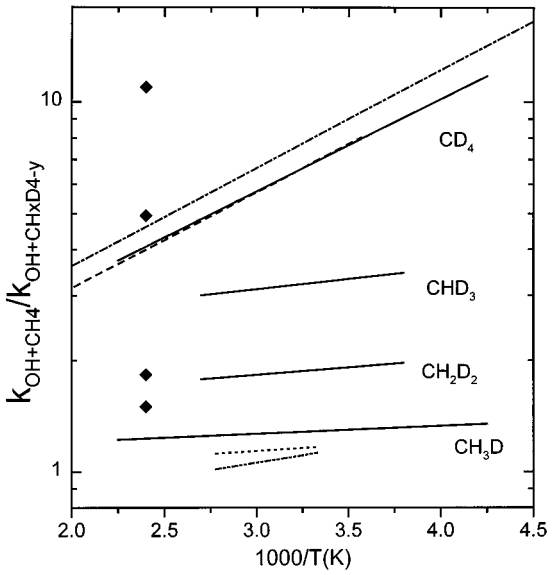

Figure 3. $k_{CH_4}/k_{CH_xD_y}$, plotted as a function of temperature. Experimental results of Gordon and Mulac are shown as diamonds for CH_3D, CH_2D_2, CHD_3, and CD_4, going from bottom to top. The solid lines are the fits to our experimental results. The two short lines for CH_3D are from DeMore[16] measured relative to HFC-134a (top line) and HCFC-141b (bottom line). The dashed line for CD_4 is the results of Dunlop and Tully.[17] The dashed line for CD_4 is the calculations of Melissas and Truhlar.[25]

is higher for k_4 than that for k_5. This difference also suggests that tunneling is important, especially for the abstraction of H atoms.

For atmospheric purposes, the quantity of interest is the ratio of the rate coefficients for the isotopic species, especially k_5/k_1. The kinetic isotope effects for four deuterated analogs of methane were calculated over the temperature range, typically 245−410 K. For convenience, the KIE values as a function of temperature were fitted to the expression KIE $= A \exp(B/T)$. The resulting A and B parameters are shown in Table 5. These parameters reproduce the measured ratios to approximately 10%. The results from this study along with those from other groups are summarized in Table 5 and Figure 3.

The present result (1.23 ± 0.09 at 298 K) for k_5/k_1 is to be compared with DeMore's value[16] at 298 K of 1.15 (an average from two relative measurements where different reference compounds were used). The kinetic isotope effect (KIE) measured by DeMore slowly decreases with increasing temperature, in agreement with the trend in our results. Gordon and Mulac[15] measured the KIE in the reaction of OH with CH_3D vs CH_4 at 416 K, which is listed in Table 5. For atmospheric purposes, it is best to measure k_1/k_5 in a relative rate study. Unfortunately, however, DeMore could not carry out such a measurement because of experimental difficulties.[16] Therefore, he measured the rate coefficients for the reactions of OH with CH_4 and CH_3D relative to HFC-134a and HCFC-141b as standards. This use of a "transfer standard" introduces additional imprecision. Further, DeMore's measured ratios of k_1/k_5 are different for the two different standards. He pointed out that the results using the HFC-134a as a transfer standard are to be preferred. Alternatively, the difference between the two sets of results may be viewed as an indicator of the precision of the measurement. In any case, the difference in the measured ratios of the rate constants could be significant for atmospheric calculations.

The ratio k_5/k_1 has also been calculated to be 1.18 using the BEBOVIB-IV method[7] and 1.33 using an *ab initio* method.[23] Even though these numbers appear to be close to the measured values, the differences are large because a large number of factors should cancel out in KIE calculations. Further improvements in such calculations are clearly needed.

Previously, only Gordon and Mulac[15] had reported the rate coefficients for the reactions of OH with CH_2D_2 and CHD_3 at 416 K. The isotope effect calculated from their data is listed in Table 5.

The ratio k_5/k_4 was measured by Dunlop and Tully[17] in the temperature range of 800−298 K. Their 298 K value for KIE is 7.07 (calculated from the fit), in excellent agreement with our value of 7.19. Further, the temperature dependence of this KIE seen by Dunlop and Tully is in excellent agreement with ours (see Figure 3). From our experiments, as well as from those of Dunlop and Tully, the kinetic isotope effect at 416 K is calculated to be 4.00. This disagrees with the KIE derived from the work of Gordon and Mulac.[15]

Recently, Melissas and Truhlar,[24,25] and Hu *et al.*,[26] computed $k_5(T)$, $k_4(T)$, and k_5/k_4 using the variational transition-state theory with multidimensional tunneling corrections (CVT/SCT) and an *ab initio* potential energy surface. The calculated values of Melissas and Truhlar are systematically higher than our experimental data. Hu *et al.*[26] also report values of k_5 and k_4 at several temperatures. They attempted to match the calculated rate constants as well as the KIE with observations. In general, their calculated values of k_5 agree better with experimental data than that does k_4. Again, these comparisons show that improvements in calculations are needed.

When OD is used in place of OH, we expect a secondary kinetic isotope effect in the rate coefficients for reactions with CH_4 (or any other methanes). Changes in the transition state for substituted and nonsubstituted system are very small, and hence the magnitude of the effect is expected to be small (KIE $\approx$ 1). There is a large body of evidence to show that the secondary KIE is small in reactions where an H atom is abstracted by OH.[9,10,12,27,28] Our measured value of k_6/k_5 is close to 1. It is interesting to note that we observe this ratio to be 1.10 ± 0.04, slightly larger than 1. Note that the uncertainty in the ratio of the rate constants arises only from the precision of the measurements in k_5 and k_6. This is because all the systematic errors in k_5 and k_6 cancel out in the ratio because both were measured in the same system using the same methods. Hence the small deviation from 1 is significant. Greiner,[28] on the other hand, reported k_6/k_5 to be 0.9 at 298 K. He reported a similar secondary KIE of 0.93 for the reactions of OD and OH with C_2H_6. This is in contrast to our results and that of Paraskevopoulos and Nip,[27] who measured the rate coefficients for OD and OH reactions with n-C_4H_{10} and n-C_4D_{10} and found k_{OD}/k_{OH} to be 1.15 ± 0.09 and 1.15 ± 0.14, respectively, for these two compounds. It should be noted that Greiner's measurements were less precise and may be incapable of resolving such small differences. We have observed such small, but greater than unity, secondary KIEs in the OD/OH + H_2 reactions.[12] It appears that OD abstracts H atoms slightly faster than OH.

To check if the measured secondary KIE is consistent with our theoretical understanding of such reactions, we have calculated the ratio of the rate coefficients for the reactions of OH and OD with H_2 and with CH_4, using the conventional transition state theory.

$$OH + H_2 \rightarrow H_2O + H; \quad k_7 \tag{7}$$

$$OD + H_2 \rightarrow HDO + H; \quad k_8 \tag{8}$$

The transition state geometries and energetics for the reactions of OH with H_2 and CH_4 have been calculated and used extensively to calculate the rate coefficients. The geometries

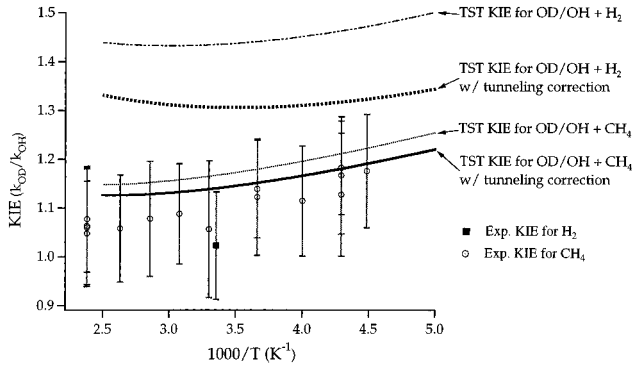

Figure 4. Plot of the calculated secondary kinetic isotope effect, k_6/k_5 or k_8/k_7 as a function of temperature. The data points are from the results of this work for the reactions of CH_4 and from Talukdar *et al.*[12] for H_2. The Appendix summarizes the parameters used in the calculations and identifies the parameters used in the calculation of the KIE for methane.

and energetics of the transition state for the OD reactions were assumed to be identical to the corresponding OH reactions. Calculations of the vibrational frequencies for the OD complexes from those of the previously reported OH complexes are given in the Appendix. Figure 4 shows the calculated ratios of the rate constants as a function of temperature for k_6/k_5 and k_8/k_7. The figure also shows the ratio of the measured values of the rate coefficients. To our knowledge, Talukdar *et al.*[12] have reported the only measurement of the rate constant for (8) and only at 298 K.

The first point to note is that these conventional transition state (CTST) calculations correctly predict that the OD reactions ((6) and (8)) are faster than the OH reactions ((5) and (7)). To assess the impact of tunneling on these reactions, we included a simple tunneling correction to the calculated rate constants using the asymptotic form of a symmetrical Eckart barrier. For both OH and OD reactions studied, the rate coefficients increased but the rate constant for the OH reaction was increased by a slightly greater amount than that for the OD reaction.

For the case of CH_4 reactions, the calculated KIE is greater than unity; i.e., OD reacts with CH_4 faster than does OH. It agrees fairly well with the observed KIE, but it overestimates the KIE. The calculated KIE for the H_2 overpredicts the KIE by a greater margin than that of CH_4. It would be useful to measure the rate coefficients for (8) as a function of temperature, especially at lower temperatures. In both cases, the prediction could benefit greatly from more comprehensive calculations of the properties of the OD−CH_4 and OD−H_2 transition states. The primary reason that OD reacts faster than OH is that the transition state is bent and the changes in the low frequencies upon D atom substitution enhances the density of states sufficiently to compensate for the differences in the densities of states in OH and OD. The lowered frequencies of the transition state decrease the barrier height by decreasing the zero-point energy in the transition state more than the increase in the barrier height due to the difference in zero-point energy between OH and OD. These changes are noted in the Appendix.

Atmospheric Implications. The tropospheric lifetimes of CH_4, CH_3D, CH_2D_2, CHD_3, and CD_4 due to reaction with OH can be estimated using the formulation of Prather and Spivakovsky[29]

$$\frac{\tau(CH_xD_y)}{\tau(CH_3CCl_3)} = \frac{k_{277\ K}(OH+CH_3CCl_3)}{k_{277\ K}(CH_xD_y)} \qquad (V)$$

to be 8.1, 10.3, 15.7, 27.7, and 66.7 years, respectively. Equation V is a good approximation because methanes and CH_3CCl_3 will be well mixed and the activation energies for their reactions with OH are not too different. For the above calculations we used a tropospheric lifetime of 4.9 years, which was recently derived from methylchloroform data collected in the ALE-GAGE program.[30] We also used the currently recommended value ($k_{277\ K}(OH+CH_3CCl_3) = 6.7 \times 10^{-15}$ cm^3 molecule^{-1} s^{-1}) for the rate coefficient for the reaction of OH with CH_3CCl_3 at 277 K.[13]

Because the primary sink for methane is due to reaction with OH there would be a large isotopic fractionation in the atmosphere. The fractionation between CH_4 vs CH_3D is very large compared to the other commonly measured isotopes, i.e., $^{12}CH_4$ vs $^{13}CH_4$. Therefore, the atmospheric levels of the deuterated isotopomers will be enhanced due to their longer lifetimes. By measuring the D/H ratio for particular methane sources and in the atmosphere, and from the measured k_1 value, the methane budget can be better constrained. The kinetic isotope effect for CH_3D vs CH_4 was evaluated from the δ(D/H) isotope budget by Tyler[7] to range between 1.17 and 1.25 with a median value of 1.21. This median value is in reasonable agreement with our results and suggests that the assumptions made by Tyler are acceptable. The weighted average temperature for removal of methane via OH reaction in the troposphere is 277 K. At this temperature, our results yield a KIE of 1.3. Even though the individual values of the rate constants measured by us agree with those of DeMore, the KIEs observed in these two studies are sufficiently different to impact the atmospheric calculations. Atmospheric model calculations should be carried out to test the sensitivities of the modeled CH_4 budgets to the KIEs.

The long lifetime of CD_4 and the absence of natural sources for this compound make it a good tracer. The long lifetime, on the other hand, also requires very long periods for the atmosphere to cleanse itself of this compound. Hence, repeated use of this compound will make CD_4 less desirable in the future.

The rate coefficient for the reaction of OH with CH_4 measured here is higher than that derived from current recommendations at temperatures close to 200 K. The larger rate constant will decrease the lifetime of CH_4 in the lower stratosphere/upper troposphere, but it will not make much difference to the atmospheric lifetime of CH_4. However, the role of OH + CH_4 reaction in affecting the OH concentration in the lower stratosphere will be larger.

Acknowledgment. This work was supported in part by NOAA's Climate and Global Change Research Program. S.C.H. held an NSF Graduate traineeship awarded to University of Colorado during part of this work.

Appendix

Summary of KIE (k_6/k_5) Calculations for the OD/OH + CH_4 Reactions. The stable geometry for the OH−CH_4 transition state and the vibrational modes were calculated previously by Truong and Truhlar.[32] Frequencies for the OD−CH_4 complex were determined by lumping the carbon and three methyl type hydrogens into a single mass 15 entity at the center of mass for that group. From this geometry, two **G** matrices were constructed corresponding to the OH−CH_4 complex and the OD−CH_4 complex. In both cases, the stable geometry[32] was used as a starting point. An arbitrary **F** matrix was generated and tweaked until it produced "reasonable" frequencies when coupled with the **G** matrix for the OH−CH_4 complex. This **F** matrix was then used with the **G** matrix for the OD−CH_4. The impact of the deuterium on the end atom was assessed and using the descriptions of the methanes modes of Dobbs and Dixon,[33] the frequencies in Table 6 were estimated for the OD−CH_4 complex.

TABLE 6: Summary of Parameters Used for KIE Calculation[a]

mode	OH−CH_4	OD−CH_4	OH	OD	CH_4
υ_1	3770	3770	3845	2797.6	3093
υ_2	3234	3234			1600
υ_3	3106	3106			3204
υ_4	1529	1529			1350
υ_5	1407	1407			
υ_6	1315	1315			
υ_7	931	931			
υ_8	827	744		⟨axial stretch⟩	
υ_9	340	340			
υ_{10}	3240	2689		⟨OH stretch⟩	
υ_{11}	1490	1028		⟨bend around O⟩	
υ_{12}	1243	1243			
υ_{13}	223	156		⟨bend around H⟩	
υ_{15}	1617*i*	1590*i*			
mass, amu	33	34	17	18	16
moments of inertia, amu Å^2					
Ia	54.9	57.1	0.916	1.73	3.17
Ib	53.9	55.5	0.916	1.73	3.17
Ic	4.14	4.93			3.17
I(IR)	0.80	1.19			
E_0, kcal/mol	6.59	6.42			

[a] Frequencies are in cm^{-1}. [b] The assignments of mode type in ⟨ ⟩ are loose descriptions. *Ab initio* prediction of the barrier height for abstraction of H from CH_4 by OH taken from Dobbs and Dixon.[33]

TABLE 7: Contributions to the Calculated KIE[a]

T (K)	n_{tran}	n_{rot}	n_{irot}	n_{vib}	n_{tun}	n_{ez}	n_{kie}	n_{kietun}
200	0.96	0.598	1.22	1.19	0.973	1.43	1.19	1.16
250	0.96	0.598	1.22	1.23	0.975	1.33	1.15	1.12
298	0.96	0.598	1.22	1.26	0.977	1.27	1.12	1.1
300	0.96	0.598	1.22	1.27	0.977	1.27	1.12	1.1
350	0.96	0.598	1.22	1.3	0.979	1.23	1.12	1.09

[a] n_{tran} is the contribution to the calculated KIE due to differences in the translational partition function. Similarly, n_{rot} refers to the rotational partition functions, n_{irot} refers to the internal rotation present in the transition states, n_{vib} refers to the vibrational partition functions, n_{tun} refers to the tunneling correction differences, and n_{ez} refers to the difference in potential energy due to differing zero-point energies. n_{kie} and n_{kietun} are the net KIE's without and with tunneling, respectively.

A Breakdown of the Results in the KIE Calculation. The contributing rotational and translational factors in the partition function (Table 7) indicate that OD reacts more slowly than OH; however, the vibrational differences between (5) and (6) suggest OD reactions would be quicker than those of OH. The presence of the extra mass at the "end" of the transition state will influence some of the vibrational modes relative to the OH−CH_4 transition state. When calculating the rate coefficient by conventional TST, these differing vibrational frequencies will influence the result in two places: the partition function and the minimum energy difference between the reactants and the transition state. The lower frequency modes typical of the heavier isotope will allow for a greater partition function, and it amounts to a contest between the ratio of the vibrational partition functions of the two transition states and the inverse ratio of the reactants. In this case, at room temperature, there is little difference between the vibrational partition functions of OH and OD, because the modes are fairly great (>2000 cm^{-1}), but owing to lower frequency modes in the transition state, a ratio greater than 1 emerges, favoring the OD−CH_4 transition state. The influence of vibration does not stop there. The difference between the zero-point energy of OH and OD is great (≈1000 cm^{-1}) and this would have the effect of increasing the energy difference between reactants and the transition state, but because the D influences several modes in the transition state, the net effect is a reduction of the barrier height.

References and Notes

(1) Houghton, J. T.; Meira Filho, L. G.; Callander, B. A.; Harris, N.; Kattenberg, A.; Maskell, K. "Climate Change 1995, The Science of Climate Change", Intergovernmental Panel on Climate Change, 1995.

(2) Cicerone, R. J.; Oremland, R. S. *Global Biogeochem. Cycles* **1988**, *2*, 299−327.

(3) Wahlen, M. *Annu. Rev. Planet. Sci.* **1993**, *21*, 407−26.

(4) Mroz, E. J. *Chemosphere* **1993**, *26*, 45−53.

(5) Fung, I.; Lerner, J.; Matthews, E.; Prather, M.; Steele, L. P.; Fraser, P. J. *J. Geophys. Res.* **1991**, *96*, 13033−13065.

(6) Levin, I.; Bergamaschi, P.; Dorr, H.; Trapp, D. *Chemosphere* **1993**, *26*, 161−177.

(7) Tyler, S. C. Kinetic Isotope Effects and Their Use in the Studying Atmospheric Trace Species: Case Study, CH_4 + OH. In *Isotope Effects in the Gas-Phase Chemistry*; Kaye, J. A., Ed.; American Chemical Society: Washington, DC, 1992; pp 390−408.

(8) Talukdar, R. K.; Burkholder, J. B.; Schmoltner, A.-M.; Roberts, J. M.; Wilson, R. R.; Ravishankara, A. R. *J. Geophys. Res.* **1995**, *100*, 14, 163−14, 173.

(9) Vaghjiani, G. L.; Ravishankara, A. R. *J. Phys. Chem.* **1989**, *93*, 1948−1959.

(10) Vaghjiani, G. L.; Ravishankara, A. R.; Cohen, N. *J. Phys. Chem.* **1989**, *93*, 7833−7837.

(11) Vaghjiani, G. L.; Ravishankara, A. R. *Nature* **1991**, *350*, 406−409.

(12) Talukdar, R. K.; Gierczak, T.; Goldfarb, L.; Rudich, Y.; Madhava Rao, B. S.; Ravishankara, A. R. *J. Phys. Chem.* **1996**, *100*, 3037−3043.

(13) DeMore, W. B.; Sander, S. P.; Golden, D. M.; Hampson, R. F.; Kurylo, M. J.; Howard, C. J.; Ravishankara, A. R.; Kolb, C. E.; Molina, M. J. "Chemical Kinetics and Photochemical Data for use in Stratospheric Modeling", Jet Propulsion Laboratory, 1994.

(14) Atkinson, R.; Baulch, D. L.; Cox. R. A.; Hampson Jr., R. F.; Kerr, J. A.; Troe, J. *J. Phys. Chem. Ref. Data* **1992**, *21*, 1125−1568.

(15) Gordon, S.; Mulac, W. A. *Int. J. Chem. Kinet.* **1975**, Symp. 1, 289−299.

(16) DeMore, W. B. *J. Phys. Chem.* **1993**, *97*, 8564−8566.

(17) Dunlop, J. R.; Tully, F. P. *J. Phys. Chem.* **1993**, *97*, 11148.

(18) Finlayson-Pitts, B. J.; Ezell, M. J.; Jayaweera, T. M.; Berko, H. N.; Lai, C. C. *Geophys. Res. Lett.* **1992**, *19*, 1371−1374.

(19) Mellouki, A.; Teton, S.; Laverdet, G.; Quilgars, A.; LeBras, G. *J. Chem. Phys.* **1994**, *91*, 473−487.

(20) Saunders, S. M.; Hughes, K. J.; Pilling, M. J.; Baulch, D. L.; Smurthwaite, P. I. Reactions of hydroxyl radicals with selected hydrocarbons of importance in atmospheric chemistry. In *Optical methods in Atmospheric Chemistry*, Platt, H. I. S. a. U., Ed.; SPIE: Bellingham, WA, 1992; Vol. 1715; pp 88−99.

(21) Sharkey, P.; Smith, I. W. M. *J. Chem. Soc., Faraday Trans.* **1993**, *84*, 631−637.

(22) Greiner, N. *J. Chem. Phys.* **1970**, *53*, 1070−1076.

(23) Xiao, X.; Tanaka, N.; Lasaga, A. C. American Geophysical Union, Spring meeting, Baltimore, MD, 1993.

(24) Melissas, V. S.; Truhlar, D. G. *J. Chem. Phys.* **1993**, *99*, 1013.

(25) Melissas, V. S.; Truhlar, D. G. *J. Chem. Phys.* **1993**, *99*, 3542−3552.

(26) Hu, W.-P.; Liu, Y.-P.; Truhlar, D. G. *J. Chem. Soc., Faraday Trans. 2* **1994**, *90*, 1715−1725.

(27) Paraskevopoulos, G.; Nip, W. S. *Can. J. Chem.* **1980**, *58*, 2146.

(28) Greiner, N. R. *J. Chem. Phys.* **1968**, *48*, 1413.

(29) Prather, M.; Spivakovsky, C. M. *J. Geophys. Res.* **1990**, *95*, 18723−18729.

(30) Prinn, R. G.; Weiss, R. F.; Miller, B. R.; Huang, J.; Alyea, F. N.; Cunnold, D. M.; Fraser, P. J.; Hartley, D. E.; Simmonds, P. G. *Science* **1995**, *269*, 187−192.

(31) Kurylo, M. J.; Huie, R. E.; Zhang, Z.; Saini, R. D.; Padmaja, S.; Liu, R.; Fahr, A.; Braun, W.; Hunter, E. P. "Gas phase reaction rate studies and gas and liquid phase absorption cross-section measurements for CFC alternatives"; Kinetics and Mechanisms for the Reactions of Halogenated Organic Compounds in the Troposphere, Halocside/AFEAS Workshop, 1993, Dublin, Ireland.

(32) Truong, T. H.; Truhlar, D. G. *J. Chem. Phys.* **1990**, *93*, 1761.

(33) Dobbs, K. D.; Dixon, D. A. *J. Chem. Phys.* **1993**, *98*, 8852.